Joint Communications and Sensing Design for Multi-Carrier MIMO Systems

Nhan Thanh Nguyen*, Nir Shlezinger†, Khac-Hoang Ngo‡, Van-Dinh Nguyen§, Markku Juntti*
*Centre for Wireless Communications, University of Oulu, P.O.Box 4500, FI-90014, Finland
†School of ECE, Ben-Gurion University of the Negev, Beer-Sheva, Israel
‡Department of Electrical Engineering, Chalmers University of Technology, Gothenburg, Sweden
§College of Engineering and Computer Science, VinUniversity, Hanoi, Vietnam

Emails: {nhan.nguyen, markku.juntti}@oulu.fi; nirshl@bgu.ac.il; ngok@chalmers.se; dinh.nv2@vinuni.edu.vn

2023 IEEE Statistical Signal Processing Workshop (SSP) | 978-1-6654-5245-8/23/$31.00 ©2023 IEEE | DOI: 10.1109/SSP53291.2023.10207952

***Abstract*—In conventional joint communications and sensing (JCAS) designs for multi-carrier multiple-input multiple-output (MIMO) systems, the dual-functional waveforms are often optimized for the whole frequency band, resulting in limited communications–sensing performance tradeoff. To overcome the limitation, we propose employing a subset of subcarriers for JCAS, while the communications function is performed over all the subcarriers. This offers more degrees of freedom to enhance the communications performance under a given sensing accuracy. We first formulate the rate maximization under the sensing accuracy constraint to optimize the beamformers and JCAS subcarriers. The problem is solved via Riemannian manifold optimization and closed-form solutions. Numerical results for an 8×4 MIMO system with 64 subcarriers show that compared to the conventional subcarrier sharing scheme, the proposed scheme employing 16 JCAS subcarriers offers 60% improvement in the achievable communications rate at the signal-to-noise ratio of 10 dB. Meanwhile, this scheme generates the sensing beampattern with the same quality as the conventional JCAS design.**

***Index Terms*—Joint communications and sensing (JCAS), dual-functional radar-communications (DFRC), MIMO-OFDM.**

I. Introduction

The increasing demand for mobile communications services has raised the cost of bandwidth and caused frequency shortage [1]. Recently, cooperative spectrum sharing among licensed radar and communications systems has emerged as a key enabler for efficient use of bandwidth [2]. Such coexisting systems are usually referred to as joint communications and sensing (JCAS) systems [3]. Early studies on JCAS focused on interference management techniques to control the mutual interference between the radar and communications subsystems [4]–[14]. Particularly, Liu *et al.* [12] proposed two JCAS operations for a multiple-input multiple-output (MIMO) downlink based on sharing array elements for the two subsystems. Hassanien *et al.* [5] proposed transmitting communications data outside the main lobes of the radar. Wu *et al.* [15] introduced a frequency-hopping MIMO radar-based waveform for channel estimation. In [16]–[19], constant-modulus waveforms were designed to avoid signal distortion in nonlinear power amplifiers.

The aforementioned works mostly focus on single-carrier transmission. However, orthogonal frequency-division multiplexing (OFDM) can achieve a higher radar and communications performance [7], [20], [21]. In single-antenna OFDM systems [22], [23], the major degrees of freedom is attained via power allocation [22] or dynamic subcarrier allocation [23]. Wu *et al.* [24] optimized the MIMO-OFDM data symbols carried by subcarriers for better time and spatial domain signal orthogonality. Johnston *el al.* [1] designed the radiated waveforms and the receive filters for MIMO-OFDM JCAS systems. More recent works [25], [26] focus on JCAS designs in massive MIMO-OFDM systems.

Based on the subcarrier sharing among radar and communications, existing JCAS designs for multi-carrier/OFDM systems can be divided into two groups, wherein the two subsystems operate at either the same [1], [3], [24], [26], [27] or distinct subcarriers [23]. Under sensing accuracy constraints, the former operation has communications performance loss across all the subcarriers, while that loss in the latter is even more significant due to the bandwidth fraction allocated for radar sensing. The higher accuracy required in sensing, the more significant performance loss occurs in communications. To overcome this, we herein propose an efficient JCAS design based on optimizing the subcarrier sharing and dual-functional beampatterns. The main idea is to allocate a subset of subcarriers for JCAS, while allowing communications over the entire bandwidth. In this way, radar sensing only interferes with data transmissions in predetermined sub-bands, while effective sensing can still be ensured with an efficient beampattern design. The communications via the remaining subcarriers are thus maximized without any effects from sensing. We formulate such a design as a rate maximization problem under sensing and power constraints. The problem is solved via subcarrier selection and Riemannian manifold optimization. Our numerical results show that the proposed JCAS scheme offers a remarkable improvement in the communications–sensing performance tradeoff with respect to the conventional counterpart.

II. Signal Model and Problem Formulation

A. Signal Model

We consider a MIMO-OFDM JCAS system, where the base station (BS) simultaneously transmits probing signals to the sensing targets at the angles of interest and data signals to

the mobile stations (MS). Let $N_{\rm t}$ and $N_{\rm r}$ denote the numbers of antennas at the BS and MS, respectively, and let $\mathcal{K} = \{1, 2, \ldots, K\}$ be the set of all employed subcarriers. Denote by $\mathbf{s}[k] \in \mathbb{C}^{N_{\rm s}\times 1}$ the transmit signal vector at subcarrier k, with $\mathbb{E}\{\mathbf{s}[k]\mathbf{s}[k]^{\rm H}\} = \mathbf{I}_{N_{\rm s}}$, where $N_{\rm s}$ is the number of data streams. We assume that while all subcarriers in $\mathcal{K}$ are used for communications, only a subset $\mathcal{J} \subset \mathcal{K}$ of $J = |\mathcal{J}|$ subcarriers are used for sensing. Accordingly, subcarriers in $\mathcal{J}$ are employed for *both communications and sensing*, and thus, are referred to as *JCAS subcarriers*.

Let $\mathbf{F}[k] \in \mathbb{C}^{N_{\rm t}\times N_{\rm s}}$ and $\mathbf{W}[k] \in \mathbb{C}^{N_{\rm r}\times N_{\rm s}}$ be the precoding matrix at the BS and the combining matrix at the MS, respectively, at subcarrier k. The power constraint at the BS is given as $\|\mathbf{F}[k]\|_{\mathcal{F}}^2 = P_{\rm BS}, \forall k$, where $\|\cdot\|_{\mathcal{F}}$ denotes the Frobenius norm, and $P_{\rm BS}$ is the power budget at the BS. After combining, the received signal at the MS is given by

$$\mathbf{y}[k] = \mathbf{W}[k]^{\rm H}\mathbf{H}[k]\mathbf{F}[k]\mathbf{s}[k] + \mathbf{W}[k]^{\rm H}\mathbf{n}[k], \tag{1}$$

where $\mathbf{n}[k] \sim \mathcal{CN}(\mathbf{0}, \sigma_{\rm n}^2\mathbf{I}_{N_{\rm r}})$ is the additive white Gaussian noise (AWGN) at the MS, and $\mathbf{H}[k] \in \mathbb{C}^{N_{\rm r}\times N_{\rm t}}$ is the channel matrix at subcarrier k. We assume that $\mathbf{H}[k]$ is known at the BS and MS. Based on (1), the achievable rate at subcarrier k of the MS is given as

$$\mathcal{R}_k = \log_2\left|\mathbf{I}_{N_{\rm r}} + \frac{P_{\rm BS}}{\sigma_{\rm n}^2 N_{\rm s}}\mathbf{W}[k]^{\dagger}\mathbf{H}[k]\mathbf{F}[k]\mathbf{F}[k]^{\rm H}\mathbf{H}[k]^{\rm H}\mathbf{W}[k]\right|, \tag{2}$$

where $|\cdot|$ and $(\cdot)^{\dagger}$ denote the determinant and pseudo-inverse of a matrix, respectively.

B. Problem Formulation

1) Radar Beampattern Design: The design of the radar beampattern is equivalent to the design of the covariance matrix of the radar probing signals, denoted as $\mathbf{R}[k]$. This can be formulated as [12], [16]

$$\underset{\{\mathbf{R}[k]\}}{\text{minimize}} \sum_{k\in\mathcal{J}}\sum_{t=1}^{T} |\mathcal{P}_{\rm d}(\theta_t, f_k) - \mathbf{a}(\theta_t, f_k)^{\rm H}\mathbf{R}[k]\mathbf{a}(\theta_t, f_k)| \tag{3a}$$

$$\text{subject to } [\mathbf{R}[k]]_{n,n} = P_{\rm BS}/N_{\rm t}, \quad n \in \{1, \ldots, N_{\rm t}\}, \tag{3b}$$

$$\mathbf{R}[k] \succeq \mathbf{0}, \mathbf{R}[k] = \mathbf{R}[k]^{\rm H}, \tag{3c}$$

where $\mathcal{P}_{\rm d}(\theta_t, f_k)$ is the desired beampattern gain for angle θ_t and subcarrier k; $\{\theta_t\}_{t=1}^T$ defines a fine angular grid of T angles covering the detection range $[-90^\circ, 90^\circ]$; $[\mathbf{R}[k]]_{n,n}$ is the n-th diagonal element of $\mathbf{R}[k]$ [26], [27]; and $\mathbf{a}(\theta_t, f_k) = [1, e^{j2\pi\frac{f_k\Delta}{c}\sin(\theta_t)}, \ldots, e^{j2\pi(N_{\rm t}-1)\frac{f_k\Delta}{c}\sin(\theta_t)}]^{\intercal}$ is the steering vector of the BS, with f_k and Δ being the is the k-th subcarrier frequency and the antenna spacing, respectively [1], [26]. Problem (3) is convex and can be solved by standard convex optimization tools such as CVX.

2) JCAS Design Problem: Let us denote $\mathbf{C}[k] = \mathbf{F}[k]\mathbb{E}\{\mathbf{s}[k]\mathbf{s}[k]^{\rm H}\}\mathbf{F}[k]^{\rm H} = \mathbf{F}[k]\mathbf{F}[k]^{\rm H}$ as the convariance matrix of the transmit signals at subcarrier k in the JCAS system. The quality of the beampattern formed by $\mathbf{F}[k]$ can be measured by the Frobenius norm $\|\mathbf{R}[k] - \mathbf{C}[k]\|_{\mathcal{F}}^2, \forall k \in \mathcal{J}$. Given $\mathbf{R}[k]$ obtained via solving (3) as the desired covariance matrix for radar sensing, we are interested in the JCAS beamforming design to (i) maximize the system per-subcarrier achievable rate and (ii) form beampatterns at subcarriers $k \in \mathcal{J}$ that match well with the radar beampattern $\mathbf{a}(\theta_t, f_k)^{\rm H}\mathbf{R}[k]\mathbf{a}(\theta_t, f_k)$. This design is formulated as

$$\underset{\{\mathbf{F}[k],\mathbf{W}[k]\}_{k\in\mathcal{K}},\mathcal{J}}{\text{maximize}} \quad \frac{1}{K}\sum_{k\in\mathcal{K}}\mathcal{R}_k \tag{4a}$$

$$\text{subject to} \quad \|\mathbf{F}[k]\|_{\mathcal{F}}^2 = P_{\rm BS}, \ \forall k, \tag{4b}$$

$$\frac{1}{J}\sum_{k\in\mathcal{J}}\|\mathbf{R}[k] - \mathbf{C}[k]\|_{\mathcal{F}}^2 \le \tau_0, \tag{4c}$$

where τ_0 is a sensing accuracy tolerance. It is noted that the set $\mathcal{J}$ of integers is also a design variable. The design in (4) is unlike most of the existing works on MIMO JCAS [12], [16], which focus on maximizing sensing accuracy under the communications performance constraints.

Our communications-centric design (4) is motivated by the fact that when a large number of subcarriers is available, a subset of them can be used for sensing and guarantee a required accuracy without directly minimizing $\sum_{k\in\mathcal{J}}\|\mathbf{R}[k] - \mathbf{C}[k]\|_{\mathcal{F}}^2$ as in [12], [16]. It offers more degrees of freedom to improve communications performance. Despite that, problem (4) is nonconvex and involves integer variables, i.e, $\mathcal{J}$. Our proposed solution to these challenges is elaborated next.

III. Proposed JCAS Design

We first note that eigenmode beamforming is not applicable for (4) due to constraint (4c). More specifically, setting $\mathbf{F}[k]$ and $\mathbf{W}[k]$ to the right and left singular vectors of $\mathbf{H}[k]$, respectively, can maximize $\mathcal{R}_k$, but cannot ensure (4c). Instead, we first design the precoders $\{\mathbf{F}[k]\}_{k\in\mathcal{K}}$ assuming that optimal combiners $\{\mathbf{W}[k]\}_{k\in\mathcal{K}}$ are used.[1] Then, we optimize $\{\mathbf{W}[k]\}$ for the designed $\{\mathbf{F}[k]\}$. Furthermore, we exploit the observation that the sensing waveform constraint does not depend on the channels $\{\mathbf{H}[k]\}_{k\notin\mathcal{J}}$, as seen from (4c). This implies that $\{\mathbf{F}[k], \mathbf{W}[k]\}$ can be designed to maximize the total rate $\sum_{k\in\mathcal{K}\setminus\mathcal{J}}\mathcal{R}_k$ over the set $\mathcal{K}\setminus\mathcal{J}$ without affecting the sensing performance. In this light, sensing has the smallest effect on communications if $\mathcal{J}$ contains subcarriers offering the smallest rates $\mathcal{R}_k$. This design strategy is outlined in the following steps:

1) Assuming optimal combiners $\{\mathbf{W}[k]\}$, solve problem

$$\underset{\{\mathbf{F}[k]\}}{\text{maximize}} \ \frac{1}{K}\sum_{k\in\mathcal{K}}\mathcal{R}_k, \ \text{subject to (4b)} \tag{5}$$

to obtain precoders $\{\hat{\mathbf{F}}[k]\}$.

2) Obtain set $\mathcal{J} \in \mathcal{K}$ containing J subcarriers associated with the smallest rates $\mathcal{R}_k$.

3) With given $\{\hat{\mathbf{F}}[k]\}$, solve the JCAS problem

$$\underset{\{\mathbf{F}[k]\},k\in\mathcal{J}}{\text{minimize}} \ \frac{\rho}{J}\sum_{k\in\mathcal{J}}\|\mathbf{F}[k]\mathbf{F}[k]^{\rm H} - \mathbf{R}[k]\|_{\mathcal{F}}^2 + \frac{\bar{\rho}}{J}\sum_{k\in\mathcal{J}}\left\|\mathbf{F}[k] - \hat{\mathbf{F}}[k]\right\|_{\mathcal{F}}^2 \tag{6a}$$

[1] In the following, we drop the subscript $k \in \mathcal{K}$ for ease of exposition.

$$\text{subject to (4b)} \tag{6b}$$

to obtain $\tilde{\mathbf{F}}[k], k \in \mathcal{J}$, where ρ is a weighting factor that balances the communications and sensing performance, and $\bar{\rho} = 1 - \rho$. Then, obtain the final precoders

$$\mathbf{F}[k] = \begin{cases} \tilde{\mathbf{F}}[k], & k \in \mathcal{J} \\ \hat{\mathbf{F}}[k], & \text{otherwise.} \end{cases} \tag{7}$$

4) With the obtained precoders $\mathbf{F}[k]$, solve problem

$$\underset{\{\mathbf{W}[k]\}}{\text{maximize}} \quad \frac{1}{K} \sum_{k \in \mathcal{K}} \mathcal{R}_k \tag{8}$$

to obtain the optimal combiners $\{\mathbf{W}[k]\}$.

Note that in problem (6), we have incorporated constraint (4c) in the objective function as a penalty term. This is to simplify the design but does not reduce its efficiency because a better sensing accuracy can be always achieved by setting a larger ρ in (6a), as will be further justified via simulations. Next, we present the solutions to subproblems (5), (6), and (8).

1) Solution to Problem (5)*:* Let $\mathbf{V}[k] \in \mathbb{C}^{N_t \times N_s}$ be the matrix consisting of N_s right singular vectors associated with the N_s largest singular values of $\mathbf{H}[k]$. Then, the optimal solution to $\mathbf{F}[k]$ is given by

$$\mathbf{F}[k] = \mathbf{V}[k]\mathbf{P}[k]^{1/2}, \tag{9}$$

where $\mathbf{P}[k]$ is a diagonal matrix with diagonal elements being water-filling power allocation factors satisfy (4b).

2) Solution to Problem (6)*:* We can rewrite (6) as

$$\underset{\{\mathbf{F}[k]\}}{\text{minimize}} \quad \frac{1}{J} \sum_{k \in \mathcal{J}} \gamma_k, \text{ subject to } \text{(4b)}, \tag{10}$$

where

$$\gamma_k \triangleq \rho \left\| \mathbf{F}[k]\mathbf{F}[k]^{\mathsf{H}} - \mathbf{R}[k] \right\|_{\mathcal{F}}^2 + \bar{\rho} \left\| \mathbf{F}[k] - \hat{\mathbf{F}}[k] \right\|_{\mathcal{F}}^2. \tag{11}$$

Since constraints (4b) for different $k \in \mathcal{J}$ are independent, problem (10) can be solved across k independently, i.e.,

$$\underset{\mathbf{F}[k] \in \mathcal{S}}{\text{minimize}} \quad \gamma_k, \tag{12}$$

where $\mathcal{S} \triangleq \{\mathbf{F}[k] \in \mathbb{C}^{N_\mathrm{t} \times N_\mathrm{s}} : \|\mathbf{F}[k]\|_{\mathcal{F}} = \sqrt{P_{\mathrm{BS}}}, \forall k \in \mathcal{J}\}$ is the complex hypershpere manifold with radius $\sqrt{P_{\mathrm{BS}}}$. This motivates a Riemannian manifold minimization [28] to efficiently find a near-optimal solution to (12). To this end, we find the Euclidean gradient of γ_k with respect to $\mathbf{F}[k]$ as

$$\nabla\gamma_k = 4\rho \left(\mathbf{F}[k]\mathbf{F}[k]^{\mathsf{H}} - \mathbf{R}[k]\right) \mathbf{F}[k] + 2\bar{\rho}\big(\mathbf{F}[k] - \hat{\mathbf{F}}[k]\big). \tag{13}$$

A tangent space corresponds to $\mathcal{S}$ is given by

$$\mathscr{T}_{\mathbf{F}[k]}\mathcal{S} = \left\{ \mathbf{F}[k] \in \mathbb{C}^{N_\mathrm{t} \times M} : \Re(\mathrm{trace}\left(\mathbf{F}[k]^{\mathsf{H}}\mathbf{F}[k]\right)) = 0 \right\},$$

where $\Re(\cdot)$ denotes the real part of a complex number. We can obtain the Riemannian gradient corresponding to the Euclidean $\nabla\gamma_k$ by projecting $\nabla\gamma_k$ onto tangent space $\mathscr{T}_{\mathbf{F}[k]}\mathcal{S}$, i.e.,

$$\begin{aligned} \mathrm{grad}\gamma_k &= \mathrm{Proj}_{\mathbf{F}[k]}\left(\nabla\gamma_k\right) \\ &= \nabla\gamma_k - \Re(\mathrm{trace}\left(\mathbf{F}[k]^{\mathsf{H}}\nabla\gamma_k\right))\mathbf{F}[k]. \end{aligned} \tag{14}$$

Algorithm 1. Proposed solution to the JCAS design (4)

Input: $\{\mathbf{H}[k], \mathcal{P}_\mathrm{d}(\theta_t, f_k), \mathbf{a}(\theta_t, f_k)\}$.
Output: $\{\mathbf{F}[k], \mathbf{W}[k]\}$.
1: Obtain $\{\mathbf{F}[k]\}$ based on (9). Set $\hat{\mathbf{F}}[k] = \mathbf{F}[k], \forall k \in \mathcal{K}$.
2: Find the set $\mathcal{J}$ of J subcarriers offering the smallest rates.
3: Solve problem (3) to obtain $\{\mathbf{R}[k]\}$.
4: **for** $k \in \mathcal{J}$ **do**
5: Set $i = 0$, initialize $\mathbf{F}[k]_{(0)}$ and $\mathbf{\Pi}_{(0)} = -\mathrm{grad}\gamma_{k(0)}$.
6: **repeat**
7: Compute stepsize $\delta_{(i)}$ by Armijo rule.
8: Update $\mathbf{F}[k]_{(i)}$ based on (15).
9: Compute $\mu_{(i)}$ based on (17).
10: Compute $\mathbf{\Pi}_{(i)}$ based on (16).
11: $i = i + 1$.
12: **until** convergence
13: **end for**
14: Set $\tilde{\mathbf{F}}[k]$ to the solutions $\mathbf{F}[k]_{(i)}$ at convergence, $k \in \mathcal{J}$.
15: Obtain final beamformers $\{\mathbf{F}[k]\}$ based on (7).
16: Obtain combiners $\{\mathbf{W}[k]\}$ based on (18).

In an iteration of the Riemannian conjugate gradient scheme, say iteration $i+1$, $\mathbf{F}[k]$ is updated as follows:

$$\begin{aligned} \mathbf{F}[k]_{(i+1)} &= \mathrm{Retract}_{\mathbf{F}[k]_{(i)}}\left(\delta_{(i)}\mathbf{\Pi}_{(i)}\right) \\ &= \frac{\sqrt{P_{\mathrm{BS}}}\left(\mathbf{F}[k]_{(i)} + \delta_{(i)}\mathbf{\Pi}_{(i)}\right)}{\left\|\mathbf{F}[k]_{(i)} + \delta_{(i)}\mathbf{\Pi}_{(i)}\right\|_{\mathcal{F}}}, \end{aligned} \tag{15}$$

where $\delta_{(i)}$ is the Armijo step-size [12], [28], and $\mathbf{\Pi}_{(i)}$ is the descent direction. Here, $\mathbf{\Pi}_{(i)}$ is derived as

$$\mathbf{\Pi}_{(i)} = -\mathrm{grad}\gamma_{k(i)} + \mu_{(i)}\mathcal{T}_{\mathbf{F}[k]_{(i-1)}}\big(\mathbf{\Pi}_{(i-1)}\big), \tag{16}$$

where $\mathrm{grad}\gamma_{k(i)}$ is the Riemannian gradient $\mathrm{grad}\gamma_k$ at $\mathbf{F}[k] = \mathbf{F}[k]_{(i)}$, and $\mathcal{T}_{\mathbf{F}[k]_{(i-1)}}(\mathbf{\Pi}_{(i-1)}) = \mathrm{Proj}_{\mathbf{F}[k]_{(i)}}(\mathbf{\Pi}_{(i-1)})$ transports $\mathbf{\Pi}_{(i-1)} \in \mathscr{T}_{\mathbf{F}[k]_{(i-1)}}\mathcal{S}$ to the tangent space $\mathscr{T}_{\mathbf{F}[k]_{(i)}}\mathcal{S}$ using the projection defined in (14), and $\mu_{(i)}$ is computed as

$$\mu_{(i)} = \frac{\langle \mathrm{grad}\gamma_{k(i)}, \overline{\mathrm{grad}}\gamma_{k(i)} \rangle}{\langle \mathrm{grad}\gamma_{k(i-1)}, \mathrm{grad}\gamma_{k(i-1)} \rangle}, \tag{17}$$

with $\langle \mathbf{X}, \mathbf{Y} \rangle \triangleq \Re(\mathrm{trace}\left(\mathbf{X}^{\mathsf{H}}\mathbf{Y}\right))$ and $\overline{\mathrm{grad}}\gamma_{k(i)} \triangleq \mathrm{grad}\gamma_{k(i)} - \mathscr{T}_{\mathbf{F}[k]_{(i-1)}}\left(\mathrm{grad}\gamma_{k(i)}\right)$.

3) Solution to Problem (8)*:* Given $\mathbf{F}[k]$, the optimal solution to $\mathbf{W}[k]$ is given as

$$\mathbf{W}[k] = \mathbf{U}[k], \tag{18}$$

where $\mathbf{U}[k]$ consists of N_s left singular vectors corresponding to the N_s largest singular values of $\mathbf{H}[k]\mathbf{F}[k]$.

4) Overall Proposed JCAS Design: The proposed design for the considered JCAS problem is outlined in Algorithm 1. Specifically, $\{\hat{\mathbf{F}}[k]\}$ are first obtained in step 1 for the maximum communications rates via all subcarriers. In step 2, we solve the benchmark covariance matrices $\{\mathbf{R}[k]\}$, which are then used in steps 4–14 to find $\{\tilde{\mathbf{F}}[k]\}$ based on the Riemannian manifold optimization detailed in Section III-2. The final beamformers and combiners are obtained in steps 15 and 16, respectively.

5) Complexity Analysis: We end this section with a complexity analysis of the proposed algorithm. The complexity of obtaining $\{\mathbf{F}[k]\}$ in (9) is $K\mathcal{O}(N_\mathrm{t}N_\mathrm{r}^2)$, dominated by the sin-

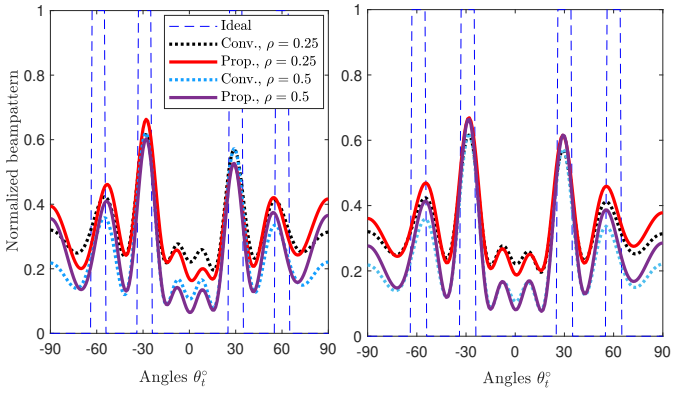

(a) $J = 16$ (b) $J = 32$

Fig. 1. Beampatterns of the proposed and conventional JCAS schemes with $\rho = \{0.25, 0.5\}$, $J = \{16, 32\}$, and SNR $= 10$ dB.

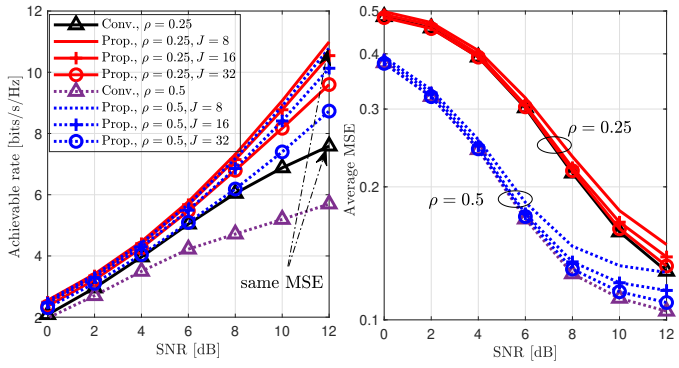

(a) Rate vs. SNR (b) MSE vs. SNR

Fig. 2. Achievable rates and MSEs of the proposed and conventional JCAS schemes with $\rho = \{0.25, 0.5\}$ and $J = \{8, 16, 32\}$.

gular value decomposition (SVD) of $\{\mathbf{H}[k]\}$. The complexity of the Riemannian manifold minimization is $J\mathcal{O}(4N_{\mathrm{t}}^2N_{\mathrm{s}} + 3N_{\mathrm{t}})$, which is mostly to compute the Euclidean gradient in (13) [12]. Finally, solving $\{\mathbf{W}[k]\}$ requires performing multiplication and SVD of $\{\mathbf{H}[k]\mathbf{F}[k]\}$ with a complexity of $K\mathcal{O}(2N_{\mathrm{t}}N_{\mathrm{r}}N_{\mathrm{s}} + N_{\mathrm{r}}^2N_{\mathrm{s}})$. Therefore, the overall complexity of Algorithm 1 is $\mathcal{O}(4JN_{\mathrm{t}}^2N_{\mathrm{s}} + KN_{\mathrm{t}}N_{\mathrm{r}}^2 + 2KN_{\mathrm{t}}N_{\mathrm{r}}N_{\mathrm{s}} + KN_{\mathrm{r}}^2N_{\mathrm{s}})$.

IV. Simulation Results

We herein provide numerical results to demonstrate the efficiency of the proposed JCAS design. In the simulations, we set $N_{\mathrm{t}} = 8$, $N_{\mathrm{r}} = 4$, $K = 64$, $\sigma_{\mathrm{n}}^2 = 1$, and $f_k = f_0 + (k-1)\Delta f$, where $f_0 = 2$ GHz and $\Delta f = 100$ kHz [1]. We assume the deployment of a uniform linear array (ULA) with antenna spacing $\Delta = c/(2f_K)$ [1], where $c \approx 3 \times 10^8$ m/s is the speed of light. We adopt the Rayleigh fading model for the channels $\mathbf{H}[k], \forall k \in \mathcal{K}$ [12]. The sensing targets are assumed to be located at angles $\theta_{\mathrm{d}} \in \{-60^\circ, -30^\circ, -30^\circ, 60^\circ\}$, and the corresponding desired beampattern is defined as [26]

$$\mathcal{P}_{\mathrm{d}}(\theta_t, f_k) = \begin{cases} 1, & \theta_t \in [\theta_{\mathrm{d}} - \delta_\theta, \theta_{\mathrm{d}} + \delta_\theta] \\ 0, & \text{otherwise} \end{cases}, \quad \forall k, \tag{19}$$

where $\delta_\theta = 8$ is the half of the mainlobes of $\mathcal{P}_{\mathrm{d}}(\theta_t, f_k)$. The Riemannian manifold optimization is implemented using the

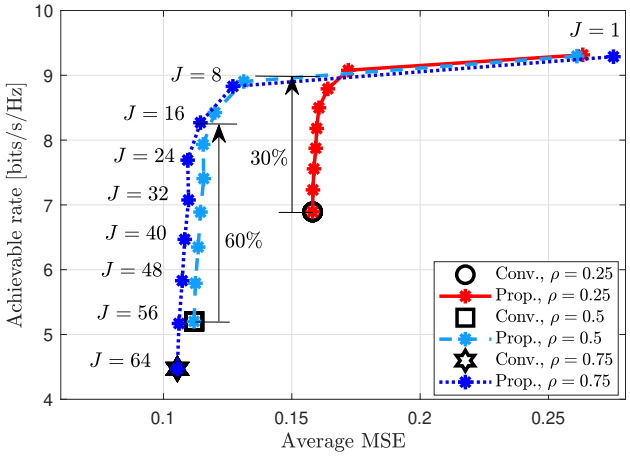

Fig. 3. Communications-sensing performance tradeoff of the proposed JCAS scheme with $\rho = \{0.25, 0.5, 0.75\}$, $J = \{1, 8, 16, \ldots, K\}$, SNR $= 10$ dB.

Manopt toolbox [29]. All the results are averaged over 100 channel realizations. In the figures, the term "Prop." refers to the proposed JCAS design with $J < K$, while the conventional design with $J = K$ is referred to as "Conv."

In Fig. 1, we plot the beampatterns obtained by the proposed JCAS design with $J = \{16, 32\}$ in comparison to those of the conventional setup, i.e., $J = K$, as well as the ideal beampattern in (19). For problem (6), we consider moderate weighting factors of $\rho = \{0.25, 0.5\}$. It is observed that despite the reduced number of JCAS subcarriers, the proposed scheme still forms good beampatterns with peaks located at desired detection angles θ_{d}, and they are as high as those of the conventional beampatterns. Around the margin angles $\{\pm 90^\circ\}$, the proposed beampatterns exhibit a higher error than the conventional ones, which can be reduced by increasing J, as seen for the case $J = 32$. When ρ increases, the power distributes less over sidelobe angles $\theta_t \notin \{-60^\circ, -30^\circ, -30^\circ, 60^\circ\}$. This enhances the peak-to-sidelobe ratio (PSLR) and improves the sensing accuracy [12], [16] but essentially degrades the communications performance, as shown next.

In Fig. 2, we compare the achievable communications rates and the average sensing beampattern mean squared errors (MSEs) of the considered JCAS schemes versus SNRs (defined as $P_{\mathrm{BS}}/\sigma_{\mathrm{n}}^2$) for $\rho = \{0.25, 0.5\}$ and $J = \{8, 16, 32\}$. Here, the average beampattern MSE is defined as $\mathrm{MSE} = \frac{1}{JT}\sum_{k\in\mathcal{J}}\sum_{t=1}^{T}|\mathcal{P}_{\mathrm{d}}(\theta_t, f_k) - \mathbf{a}(\theta_t, f_k)^{\mathrm{H}}\mathbf{C}[k]\mathbf{a}(\theta_t, f_k)|^2$. It is seen that for the same ρ, the proposed JCAS design achieves remarkable rate improvement with only a marginal loss in the MSE. In particular, the improvement is more significant with a larger ρ, which is reasonable because the proposed subcarrier sharing plays a more important role under strict sensing constraints. This implies that employing a larger ρ and a smaller J should be employed for better communication–sensing performance tradeoff. As an example, at SNR $= 12$ dB, the proposed scheme with $\rho = 0.5$ and $J = 8$ achieves 42.4% higher rate while maintaining the same MSE ($= 0.128$) as the conventional scheme with $\rho = 0.25$ and $J = K$.

We further demonstrate the superior tradeoff improvement of the proposed scheme in Fig. 3 by showing the

communications rate versus the MSEs obtained for $J = \{1, 8, 16, \ldots, 64\}$, $\rho = \{0.25, 0.5, 0.75\}$, and SNR $= 10$ dB. It is seen for the proposed scheme that as J increases, both the MSEs and communications rates decrease to reach those of the conventional one. However, for a sufficiently large J, e.g., $J \geq 16$, the curves of the proposed scheme almost align with vertical lines along the y-axis. This clearly shows that the proposed JCAS design remarkably improves the communications rates while maintaining the sensing performance. For example, with $J = 16$, $\rho = 0.75$, and for the same sensing MSE $= 0.11$, the proposed scheme offers an improvement of 60% in rate performance as the conventional scheme with $J = K$ and $\rho = 0.0.5$.

V. Conclusion

We have investigated JCAS design in a MIMO-OFDM system. Aiming at maximizing the achievable communications rate while ensuring sensing accuracy, we have proposed an efficient beamforming design with a new subcarrier allocation strategy. Specifically, we proposed to use a subset of subcarriers for radar sensing, while leveraging all the available subcarriers for communications. Numerical results show that reliable sensing beampatterns can still be achieved with a reduced number of subcarriers, while the communications performance is dramatically improved. Equivalently, the communications-sensing performance tradeoff has been improved remarkably.

Aknowledgement

This research was supported by Academy of Finland under 6G Flagship (grant 346208), Infotech Oulu, and Business Finland, Keysight, MediaTek, Siemens, Ekahau and Verkotan via project 6GLearn.

References

[1] J. Johnston, L. Venturino, E. Grossi, M. Lops, and X. Wang, "MIMO OFDM dual-function radar-communication under error rate and beampattern constraints," *IEEE J. Sel. Areas Commun.*, vol. 40, no. 6, pp. 1951–1964, 2022.

[2] J. A. Zhang, F. Liu, C. Masouros, R. W. Heath, Z. Feng, L. Zheng, and A. Petropulu, "An overview of signal processing techniques for joint communication and radar sensing," *IEEE J. Sel. Topics Signal Process.*, vol. 15, no. 6, pp. 1295–1315, 2021.

[3] J. A. Zhang, X. Huang, Y. J. Guo, J. Yuan, and R. W. Heath, "Multibeam for joint communication and radar sensing using steerable analog antenna arrays," *IEEE Trans. Veh. Technol.*, vol. 68, no. 1, pp. 671–685, 2018.

[4] A. Hassanien, M. G. Amin, Y. D. Zhang, and F. Ahmad, "Signaling strategies for dual-function radar communications: An overview," *IEEE Aerosp. Electron. Syst. Mag.*, vol. 31, no. 10, pp. 36–45, 2016.

[5] ——, "Dual-function radar-communications: Information embedding using sidelobe control and waveform diversity," *IEEE Trans. Signal Process.*, vol. 64, no. 8, pp. 2168–2181, 2015.

[6] X. Liu, T. Huang, N. Shlezinger, Y. Liu, J. Zhou, and Y. C. Eldar, "Joint transmit beamforming for multiuser MIMO communications and MIMO radar," *IEEE Trans. Signal Process.*, vol. 68, pp. 3929–3944, 2020.

[7] D. Ma, N. Shlezinger, T. Huang, Y. Liu, and Y. C. Eldar, "Joint radar-communication strategies for autonomous vehicles: Combining two key automotive technologies," *IEEE Signal Process. Mag.*, vol. 37, no. 4, pp. 85–97, 2020.

[8] A. R. Chiriyath, B. Paul, and D. W. Bliss, "Radar-communications convergence: Coexistence, cooperation, and co-design," *IEEE Trans. on Cogn. Commun. Netw.*, vol. 3, no. 1, pp. 1–12, 2017.

[9] L. Zheng, M. Lops, Y. C. Eldar, and X. Wang, "Radar and communication coexistence: An overview: A review of recent methods," *IEEE Signal Process. Mag.*, vol. 36, no. 5, pp. 85–99, 2019.

[10] B. Li, A. P. Petropulu, and W. Trappe, "Optimum co-design for spectrum sharing between matrix completion based MIMO radars and a MIMO communication system," *IEEE Trans. Signal Process.*, vol. 64, no. 17, pp. 4562–4575, 2016.

[11] A. F. Martone, K. A. Gallagher, and K. D. Sherbondy, "Joint radar and communication system optimization for spectrum sharing," in *IEEE Radar Conf.*, 2019, pp. 1–6.

[12] F. Liu, C. Masouros, A. Li, H. Sun, and L. Hanzo, "MU-MIMO communications with MIMO radar: From co-existence to joint transmission," *IEEE Trans. Wireless Commun.*, vol. 17, no. 4, pp. 2755–2770, 2018.

[13] F. Liu, C. Masouros, A. Li, and T. Ratnarajah, "Robust MIMO beamforming for cellular and radar coexistence," *IEEE Trans. Wireless Commun.*, vol. 6, no. 3, pp. 374–377, 2017.

[14] S. Buzzi, C. D'Andrea, and M. Lops, "Using massive MIMO arrays for joint communication and sensing," in *Proc. Annual Asilomar Conf. Signals, Syst., Comp.*, Pacific Grove, CA, USA, 2019, pp. 5–9.

[15] K. Wu, J. A. Zhang, X. Huang, Y. J. Guo, and R. W. Heath, "Waveform design and accurate channel estimation for frequency-hopping MIMO radar-based communications," *IEEE Trans. Commun.*, vol. 69, no. 2, pp. 1244–1258, 2020.

[16] F. Liu, L. Zhou, C. Masouros, A. Li, W. Luo, and A. Petropulu, "Toward dual-functional radar-communication systems: Optimal waveform design," *IEEE Trans. Signal Process.*, vol. 66, no. 16, pp. 4264–4279, 2018.

[17] B. Tang and P. Stoica, "MIMO multifunction RF systems: Detection performance and waveform design," *IEEE Trans. Signal Process.*, vol. 70, pp. 4381–4394, 2022.

[18] W. Wu, B. Tang, and X. Wang, "Constant-modulus waveform design for dual-function radar-communication systems in the presence of clutter," *IEEE Trans. Aerosp. Electron. Syst.*, 2023.

[19] R. Liu, M. Li, Q. Liu, and A. L. Swindlehurst, "Dual-functional radar-communication waveform design: A symbol-level precoding approach," *IEEE J. Sel. Topics Signal Process.*, vol. 15, no. 6, pp. 1316–1331, 2021.

[20] M. F. Keskin, H. Wymeersch, and V. Koivunen, "MIMO-OFDM joint radar-communications: Is ICI friend or foe?" *IEEE J. Sel. Topics Signal Process.*, vol. 15, no. 6, pp. 1393–1408, 2021.

[21] C. Sturm and W. Wiesbeck, "Waveform design and signal processing aspects for fusion of wireless communications and radar sensing," *Proc. IEEE*, vol. 99, no. 7, pp. 1236–1259, 2011.

[22] A. Ahmed, Y. D. Zhang, A. Hassanien, and B. Himed, "OFDM-based joint radar-communication system: Optimal sub-carrier allocation and power distribution by exploiting mutual information," in *Proc. Annual Asilomar Conf. Signals, Syst., Comp.*, Pacific Grove, CA, USA, 2019, pp. 559–563.

[23] M. Bică and V. Koivunen, "Multicarrier radar-communications waveform design for RF convergence and coexistence," in *Proc. IEEE Int. Conf. Acoust., Speech, Signal Processing*, Brighton, UK, 2019, pp. 7780–7784.

[24] K. Wu, J. A. Zhang, Z. Ni, X. Huang, Y. J. Guo, and S. Chen, "Joint communications and sensing employing optimized MIMO-OFDM signals," *arXiv preprint arXiv:2208.09791*, 2022.

[25] M. Temiz, E. Alsusa, and M. W. Baidas, "A dual-function massive MIMO uplink OFDM communication and radar architecture," *IEEE Trans. Cogn. Commun. Netw.*, vol. 8, no. 2, pp. 750–762, 2021.

[26] Z. Cheng, Z. He, and B. Liao, "Hybrid beamforming design for ofdm dual-function radar-communication system," *IEEE J. Sel. Topics Signal Process.*, vol. 15, no. 6, pp. 1455–1467, 2021.

[27] A. M. Elbir, K. V. Mishra, and S. Chatzinotas, "Terahertz-band joint ultra-massive mimo radar-communications: Model-based and model-free hybrid beamforming," *IEEE J. Sel. Topics Signal Process.*, vol. 15, no. 6, pp. 1468–1483, 2021.

[28] X. Yu, J.-C. Shen, J. Zhang, and K. B. Letaief, "Alternating minimization algorithms for hybrid precoding in millimeter wave MIMO systems," *IEEE J. Sel. Topics Signal Process.*, vol. 10, no. 3, pp. 485–500, 2016.

[29] N. Boumal, B. Mishra, P.-A. Absil, and R. Sepulchre, "Manopt, a Matlab toolbox for optimization on manifolds," *Journal of Machine Learning Research*, vol. 15, no. 42, pp. 1455–1459, 2014. [Online]. Available: https://www.manopt.org